Single-photon pump

K. D. Osborn[a] and M. W. Keller
National Institute of Standards and Technology, 325 Broadway, Boulder, Colorado 80305

(Received 2 February 2006; accepted 27 June 2006; published online 25 August 2006)

The authors describe a gated quantum dot device called a single-photon pump that produces single photons on demand through the controlled tunneling of individual electrons and holes. Simulations using an InGaAs/GaAs dot show that two modes of operation are possible, with one mode particularly attractive for quantum cryptography applications because it cannot produce more than one photon per cycle. [DOI: 10.1063/1.2336616]

For a given mean photon number, a single-photon source (SPS) produces pulses with a smaller ratio of multiple-photon to single-photon pulses than a conventional source which is governed by Poisson statistics. Such sources are desirable for quantum key distribution systems, where security is enhanced by encoding information only in single-photon pulses since additional photons could be intercepted with impunity. One attractive type of SPS is a single-photon turnstile (SPT), which uses cyclical biasing across the *p*- and *n*-type electrodes of a *p*-*i*-QD-*i*-*n* structure to produce photons.[1] This device uses electrical control of Coulomb blockade in a quantum dot (QD) to allow sequential tunneling of an electron and a hole, which recombine to produce a single photon. Realizations of this idea have used an etched QD (Ref. 2) and an InGaAs/GaAs self-assembled QD,[3] with the latter type of QD particularly promising since the quantum efficiency is known to be high from photoluminescence data. In addition, recent single-electron transistor experiments demonstrate that individual electrons can be controllably tunneled onto InGaAs/GaAs QDs.[4,5]

In this letter we introduce a device we call the single-photon pump (SPP), shown in Fig. 1(d). The SPP consists of an InGaAs/GaAs QD separated from *n*- and *p*-type layers by intrinsic GaAs tunnel barriers, as well as a metallic gate capacitively coupled to the QD. As with the SPT, the forward-bias voltage V of the SPP can be used to raise or lower the energy of both electrons (in the *n* layer) and holes (in the *p* layer) with respect to the corresponding QD energy levels. Unlike the SPT, the gate voltage V_g of the SPP can be used to raise electron energies while lowering hole energies or vice versa. This allows for two modes of operation, forward triggered (FT) and gate triggered (GT), in which Coulomb blockade is used to controllably tunnel an electron and a hole onto the QD and thus generate a photon on demand. The former is similar to that used for the SPT, while the latter has a significant advantage that we quantify below.

Both modes can begin with V and V_g biased such that the device reaches equilibrium with one hole on the QD, as shown in the band diagram of Fig. 1(a). Here the diagram is schematic to show the individual QD levels more clearly, and below we present the actual calculations. The electron addition energy for the QD is $\mu_e(N_e,N_h)$, where N_e electrons and N_h holes are on the QD *after* the tunneling process. Similarly, the hole addition energy is $\mu_h(N_e,N_h)$. Since the line $\mu_h(0,1)$ is slightly above the Fermi energy of the *p*-type layer μ_p, a first hole can tunnel onto the QD. The lines corresponding to an electron tunneling before or after the first hole, $\mu_e(1,0)$ and $\mu_e(1,1)$, respectively, are above the filled states of the *n*-type layer, so that these processes are not allowed at this bias condition.

In the FT mode, V_g is fixed and V is changed to allow an electron to tunnel, as shown in Fig. 1(c). This is similar to the operation of a SPT, but with additional tunability from V_g that can be used to optimize device behavior. An imperfection of this FT mode bias point is that after recombination the empty QD is not stable. Another hole may tunnel *inelastically* with the emission of a phonon[6] as shown by the dashed arrow, followed by elastic tunneling of another electron and emission of another photon. This process will produce additional photons as long as the device is held at this bias condition.

In the GT mode, V is fixed and V_g is changed to allow an electron to tunnel, with a band diagram as in Fig. 1(b). The salient feature of the GT mode is that the QD is stable after recombination at this bias condition, as indicated by the crossed-out arrow showing the forbidden hole tunneling pro-

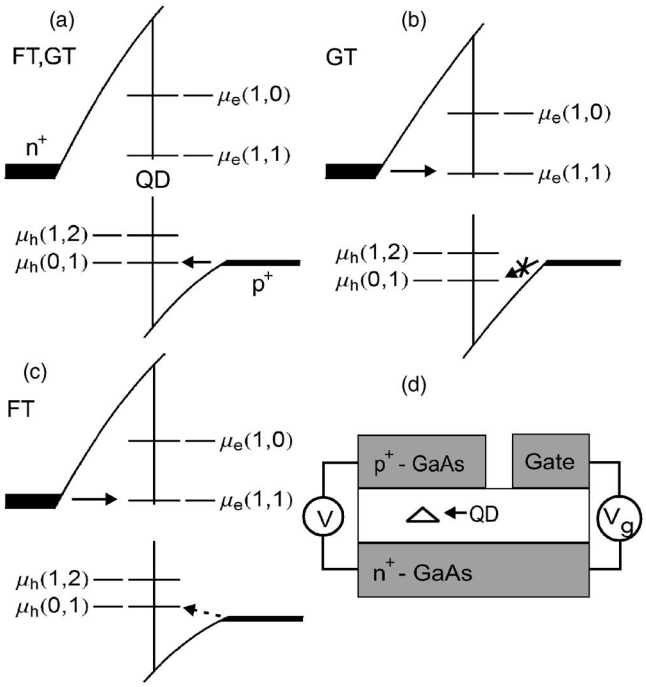


FIG. 1. Schematic band diagrams: (a) and (b) show gate-triggered (GT) operation; (a) and (c) show forward-triggered (FT) operation. μ_e and μ_h are electron and hole addition energies. Device structure is shown in (d).

[a]Electronic mail: osborn@boulder.nist.gov

Downloaded 05 Oct 2010 to 132.163.130.218. Redistribution subject to AIP license or copyright; see http://apl.aip.org/about/rights_and_permissions

cess. As a result the GT mode produces no more than one photon per bias cycle. In the rest of the letter we present quantitative simulations of both FT and GT operations for an InGaAs/GaAs QD.

The addition energies for electrons and holes are

$$\mu_e(N_e,N_h) = \varepsilon_e(V,V_g) + (N_e - 1)J_{e\text{-}e} - N_h J_{e\text{-}h} \tag{1a}$$

$$\mu_h(N_e,N_h) = \varepsilon_h(V,V_g) - (N_h - 1)J_{h\text{-}h} + N_e J_{e\text{-}h}, \tag{1b}$$

where ε_e and ε_h are the ground state orbital energies for electrons and holes, and $J_{e\text{-}e}$, $J_{e\text{-}h}$, and $J_{h\text{-}h}$ are the electron-electron, electron-hole, and hole-hole Coulomb interactions. In a typical InGaAs/GaAs QD these interactions satisfy $J_{h\text{-}h} > J_{e\text{-}h} > J_{e\text{-}e}$, and the schematic levels in Fig. 1 are drawn for this case. In order to simulate a typical quantum dot we use $J_{e\text{-}e}=28$ meV, $J_{e\text{-}h}=35$ meV, and $J_{h\text{-}h}=38.5$ meV, with a QD gap of $\varepsilon_e - \varepsilon_h = 1.27$ eV offset by a 60/40 split from the bulk GaAs band gap of $E_g=1.52$ eV. We simulate the device at zero temperature, which is applicable for thermal energies much less than the ~5 meV barrier for producing errors at our bias points.

The tunneling barriers are 15 and 20 nm thick above and below the QD, respectively. The device is simulated with negligible band bending and so the QD potential V_{QD} shifts linearly with V. In addition, we assume that V_{QD} shifts linearly with V_g, according to the geometric constant $\eta_g = \partial V_{QD}/\partial V_g|_{V}$, which was found to be ~0.02 in a comparable structure.[4,5] The n- and p-type layers are degenerately doped at $2\times10^{18}/\mathrm{cm}^3$ and $5\times10^{17}/\mathrm{cm}^3$, respectively, and the effective mass is set to $0.067m_e$ for electrons and $0.5m_e$ for holes.

To calculate the tunneling rates between the doped layers and the QD, we use the three-dimensional to zero-dimensional Bardeen tunneling formula[7] with a Wentzel-Kramers-Brillouin approximation. The effect of V_g on the band diagram is approximated as a quadratic potential between the p- and n-type layers that satisfies the boundary conditions. Since quantitative theories for inelastic tunneling are complex, we simply set the inelastic rate equal to 0.01 times the elastic rate for a particle at the Fermi energy of the electron or hole reservoir. This accounts for single-phonon emission similar to that found in GaAs resonant tunneling diodes[6] for small energy losses and gives a high inelastic tunneling rate for small barriers, as expected. The tunneling and recombination events for the device operation shown below are calculated by Monte Carlo simulation, using the calculated tunneling rates and an electron-hole recombination time constant of 300 ps, which is less than the tunneling times found in this simulation. Since electrons and holes do not exit the QD through the opposite side from which they tunneled on, the photon emission rate is related to the current I by $\Gamma_{ph}=I/e=6250\times I/(\mathrm{fA\ s})$.

The stability diagram for the SPP is shown in Fig. 2. The threshold for each electron tunneling process is marked with a negatively sloped solid line, where $\mu_n=\mu_e(N_e,N_h)$. Similarly, the threshold for each hole tunneling process is marked with a positively sloped solid line, where $\mu_p=\mu_h(N_e,N_h)$. For holes, a dashed line above the solid line of the same color indicates where the tunneling becomes only inelastic for that process. For example, above the green solid line a hole can tunnel onto an empty QD, and if the bias is also above the red solid line an electron can subsequently tunnel. After recombination, this process can repeat, causing a

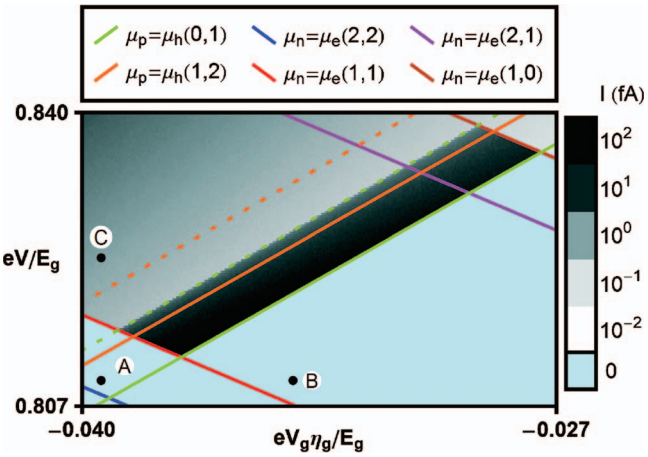


FIG. 2. (Color) Stability diagram for the SPP, showing dc current and thresholds for tunneling processes.

steady-state current to flow. Above the green dashed line, the valence band of the p-type layer $E_{VB,p}$ is greater than $\mu_h(0,1)$, and the hole can only tunnel inelastically, which reduces the current. The current is also reduced above the brown line, since the electron generally tunnels before the hole, and the hole must then tunnel inelastically. These four lines create a parallelogram of relatively high current, where both electrons and holes tunnel elastically.

Simulated operation in the GT mode involves switching between points A and B in Fig. 2 by driving V_g with the wave form of period T_p shown in the upper panel of Fig. 3. The cycle begins with no electrons or holes on the QD, where $t=0$ is chosen to be where the first hole can tunnel, $\mu_p=\mu_h(0,1)$, as point A is approached. The first hole tunnels with a nearly constant rate of $\Gamma_h=110$ kHz, giving an approximately Poissonian distribution for the probability D_{1h}

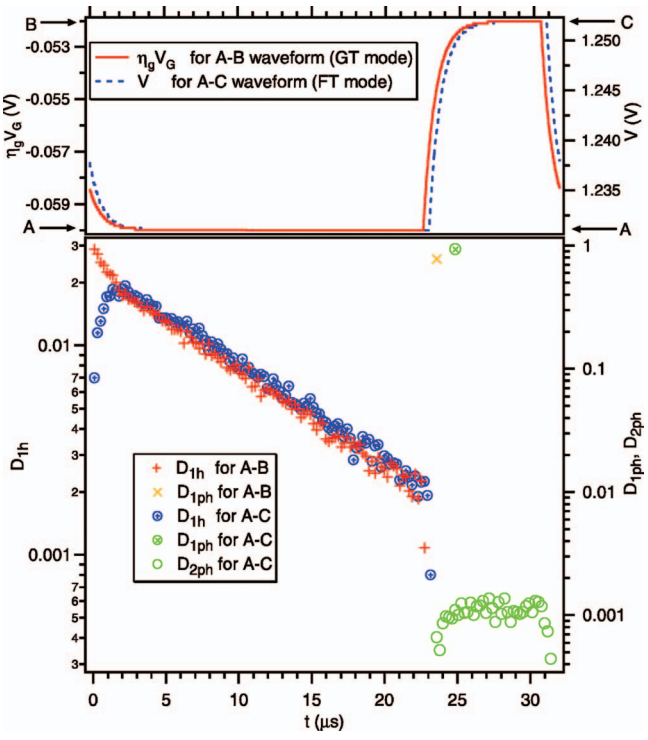


FIG. 3. (Color) Wave forms used for GT mode between points A and B and a FT cycle for points A and C (upper panel). Probability vs time for tunneling of the first hole and emission of first and second photons (lower panel).

Downloaded 05 Oct 2010 to 132.163.130.218. Redistribution subject to AIP license or copyright; see http://apl.aip.org/about/rights_and_permissions

that the first hole tunnels during the first bias point of the wave form, as shown in the lower panel of Fig. 3. As the wave form switches to point B, it passes below the line $\mu_p = \mu_h(0,1)$, where a first hole can no longer tunnel on, but if there is a hole already on the QD it can tunnel off. Electron tunneling is allowed when the line $\mu_n = \mu_e(1,1)$ is crossed. For this wave form, the probability that the hole reaches the QD before tunneling is turned off is 92% and the probability that it reaches the QD but is not lost before electron tunneling turns on is 78%. Due to the fast electron tunneling rate, $\Gamma_e = 640$ MHz, and the fast electron-hole recombination rate, the first photon in the cycle is emitted quickly with a probability of 78%, as shown by $D_{1\mathrm{ph}}$.

The salient feature of the GT mode is that at the second bias point, once a hole is no longer present due to tunneling off the QD or recombination with an electron, neither another electron nor hole can tunnel. Therefore, no more than one photon can be emitted per bias cycle. To increase the probability of emitting a single photon, the probability of tunneling a hole onto the QD can be increased by increasing the time spent at point A. Provided that the electron tunneling rate is large compared to the hole tunneling rate, the probability of emitting a single photon can be increased further by decreasing the probability that the hole tunnels off before the electron tunnels on. This can be accomplished by (1) decreasing the switching time between the two points or (2) moving bias points A and B upward, but with a V below the elastic-tunneling parallelogram, so that the time between when a hole can tunnel off and an electron can tunnel on is nearly zero.

For FT operation, we apply a wave form on V to switch between points A and C. We start with no electrons or holes on the QD and define $t=0$ when we pass below the green dashed line, where $E_{\mathrm{VB},p} = \mu_h(0,1)$, and elastic hole tunneling begins. Γ_h is initially small due to the low density of states near the band edge, and then rises to a constant value, giving a slow rise in D_{1h}, followed by an exponential decay. As we switch back to point C and cross the line $E_{\mathrm{VB},p} = \mu_h(0,1)$, holes can continue to tunnel on inelastically; however, a hole on the QD will not tunnel off. As we pass the line $\mu_n = \mu_e(1,1)$, there is a 91% probability that a hole is on the QD, and fast electron tunneling and recombination cause photon emission with the same probability ($D_{1\mathrm{ph}} = 0.91$).

After the first photon is created at point C in the FT cycle, another hole can tunnel (inelastically) followed by another electron, thus producing two (or more) photons during the cycle. With this wave form, the probability of a second photon is 4.0% per bias cycle, which is the total $D_{2\mathrm{ph}}$ shown in Fig. 3. This error probability in the FT operation can be reduced by spending less time at point C, although a time comparable to $1/\Gamma_e \sim 2$ ns would reduce the probability of producing the first photon.

In an experiment, the output statistics of the GT and FT modes for a device can be directly compared, since the output photon coupling efficiency is nearly independent of the bias point. In the GT mode, the second order correlation function at the repetition period, $g^{(2)}_{AB}(\tau = T_p)$, reaches the theoretical maximum since all of the photons are emitted precisely at multiples of T_p. In contrast, multiple-photon emission in the FT mode reduces the same quantity such that $g^{(2)}_{AC}(\tau = T_p)/g^{(2)}_{AB}(\tau = T_p) = 0.90$.

In summary, we have proposed a gated QD structure called a single-photon pump and presented simulations of two modes of operation. The gate-triggered mode is particularly attractive since it cannot produce multiple photons in one cycle. The forward-triggered mode, which is similar to the operation of a single-photon turnstile, lacks this advantage due to inelastic tunneling.

The authors acknowledge helpful discussions with R. Mirin.

[1] A. Imamoglu and Y. Yamamoto, Phys. Rev. Lett. **295**, 210 (1994).
[2] J. Kim, O. Benson, H. Kan, and Y. Yamamoto, Nature (London) **307**, 500 (1999).
[3] Z. Yuan, B. E. Kardynal, R. M. Stevenson, A. J. Shields, C. J. Lobo, K. Cooper, N. S. Beattie, D. A. Ritchie, and M. Pepper, Science **295**, 102 (2002).
[4] K. D. Osborn, M. W. Keller, and R. P. Mirin, Physica E (Amsterdam) **21**, 501 (2004).
[5] K. D. Osborn, M. W. Keller, and R. P. Mirin, *Physics of Semiconductors: 27th International Conference on the Physics of Semiconductors*, AIP Conf. Proc. No. 172 (AIP, New York, 2005), p. 819.
[6] Inelastic tunneling through the emission of phonons has been observed in resonant tunneling diodes and a model is described by N. S. Wingreen, K. W. Jacobsen, and J. Wilkins, Phys. Rev. Lett. **61**, 1396 (1988).
[7] I. Lundström and C. Svensson, J. Appl. Phys. **43**, 5045 (1972).

Downloaded 05 Oct 2010 to 132.163.130.218. Redistribution subject to AIP license or copyright; see http://apl.aip.org/about/rights_and_permissions